



Deposited via The University of Sheffield.

White Rose Research Online URL for this paper:

<https://eprints.whiterose.ac.uk/id/eprint/102596/>

Version: Accepted Version

---

**Article:**

Wu, Y., Wang, S., Liu, W. et al. (2016) Iunius: A cross layer peer-to-peer system with device-to-device communications. *IEEE Transactions on Wireless Communications*, 15 (10). pp. 7005-7017. ISSN: 1536-1276

<https://doi.org/10.1109/TWC.2016.2594225>

---

© 2016 IEEE. Personal use of this material is permitted. Permission from IEEE must be obtained for all other users, including reprinting/ republishing this material for advertising or promotional purposes, creating new collective works for resale or redistribution to servers or lists, or reuse of any copyrighted components of this work in other works

**Reuse**

Items deposited in White Rose Research Online are protected by copyright, with all rights reserved unless indicated otherwise. They may be downloaded and/or printed for private study, or other acts as permitted by national copyright laws. The publisher or other rights holders may allow further reproduction and re-use of the full text version. This is indicated by the licence information on the White Rose Research Online record for the item.

**Takedown**

If you consider content in White Rose Research Online to be in breach of UK law, please notify us by emailing [eprints@whiterose.ac.uk](mailto:eprints@whiterose.ac.uk) including the URL of the record and the reason for the withdrawal request.

# Iunius: A Cross Layer Peer-to-peer System with Device-to-device Communications

Yue Wu, Siyi Wang, Wuling Liu, Weisi Guo, and Xiaoli Chu

**Abstract**—Device-to-device (D2D) communications utilising licensed spectrum have been considered as a promising technology to improve cellular network spectral efficiency and offload local traffic from cellular base stations (BSs). In this paper, we develop Iunius: a peer-to-peer (P2P) system based on harvesting data in a community utilising multi-hop D2D communications. The Iunius system optimises D2D communications for P2P local file sharing, improves user experience, and offloads traffic from the BSs. The Iunius system features cross-layer integration of: 1) a wireless P2P protocol based on the Bittorrent protocol in the application layer; 2) a simple centralised routing mechanism for multi-hop D2D communications; 3) an interference cancellation technique for conventional cellular (CC) uplink communications; and 4) a radio resource management scheme to mitigate the interference between CC and D2D communications that share the cellular uplink radio resources while maximising the throughput of D2D communications. Simulation results show that the proposed Iunius system can increase the cellular spectral efficiency, reduce the traffic load of BSs, and improve the data rate and energy saving for mobile users.

## I. INTRODUCTION

### A. Background and Related Work

The proliferation of smartphones and tablets has dramatically stimulated the increase in mobile data traffic. It is anticipated that the mobile data demand will continue to grow exponentially in the foreseeable future, imposing a great challenge to the Long Term Evolution (LTE) and LTE-Advanced (LTE-A) systems. Device-to-device (D2D) communications underlying cellular networks, which enable two user equipments (UEs) to communicate with each other directly using the cellular radio resources, have been proposed to exploit the capacity gains offered by transmitter–receiver proximity, spectrum reuse, and multi-hop relaying [1], [2]. In future mobile networks, BSs will be busier and over longer time periods. Whether to select D2D mode or not depends on the location and channel condition of the content-requesting UE, traffic load of the BS, etc. Even when there is only one UE requesting contents, D2D transmissions would be needed if the UE is far away from the BS or its downlink is in deep fading/shadowing [1]–[3]. We note that, realising the potential advantages of D2D communications relies on effective peer discovery methods, physical layer procedures, radio resource

management (RRM) schemes and propriety multi-hop routing strategies [1]–[3].

A peer-to-peer (P2P) system enables two or more clients communicate with each other without the help from a dedicated server. Although some P2P systems (e.g., BitTorrent) require a central server to facilitate one client to find other clients, the server is not involved in actual data transmissions [4]. Conventional P2P systems usually focus on the design of application layer mechanisms without incorporating the underlying network or physical layer characteristics [4], [5]. In [6], the authors proposed a context-aware proximity-based P2P (CA-P2P) protocol, which considers the context of physical layer transmission. However, some critical information in the application layer (e.g., data storage mechanism) is missing in CA-P2P.

The infrastructureless nature of D2D communications makes it easy to integrate into the conventional P2P architecture. The wireless P2P systems proposed in [7]–[9] are based on WiFi-direct, with which efficient interference management is not available. FlashlinQ [10], [11] is a prototype P2P system based on D2D communications without considering an optimised RRM for D2D communications and an efficient P2P protocol for the system. A multicast P2P streaming application based on D2D communications was proposed in [12], where the authors focused on the node selection problem for P2P multicast considering the characteristics of D2D communications. However, many critical details, including the P2P protocol, RRM scheme and multi-hop routing algorithm are still missing in the above works. Various D2D assisted multi-media transmission systems have been proposed with distributed routing mechanisms [13], [14]. However, the fully distributed routing protocol restricts the route discovery efficiency and the coverage area over which power control can be optimised. Moreover, there is a lack of optimised RRM for multi-hop D2D communications.

In early works on RRM and interference mitigation for D2D communications underlying cellular networks [15], [16], the authors considered a simplified system containing only a single cell, one D2D pair and one CC UE. A single-cell system with an arbitrary number of CC UEs and one D2D pair was considered in [17], [18]. A resource allocation scheme was proposed in [17] to prevent the interference from CC uplink (UL) UEs to D2D communications. A power control scheme to maximise the throughput of D2D communications while guaranteeing the quality of service (QoS) requirements of CC UEs was proposed in [18]. More general scenarios consisting of multiple cells and arbitrary numbers of CC UEs and D2D pairs were considered in [19]–[21]. For D2D communications

Yue Wu, Wuling Liu and Xiaoli Chu are with the Department of Electronic and Electrical Engineering, The University of Sheffield, UK, e-mail: {yue.wu, wuling.liu, x.chu}@sheffield.ac.uk.

Siyi Wang is with the Department of Electronic and Electrical Engineering, Xi'an Jiaotong-Liverpool University, China

Weisi Guo is with the School of Engineering, University of Warwick, UK, e-mail: weisi.guo@warwick.ac.uk

underlying orthogonal frequency division multiple access (OFDMA) systems, a centralised scheme for joint resource allocation and power control and a semi-distributed one were proposed in [19] and [20], respectively. A joint resource allocation and power control scheme for D2D communications underlying single-carrier frequency division multiple access (SC-FDMA) systems was studied in [21].

## B. Contribution

It has been observed that there are often some popular and frequently requested files in a local area network during a period of time. Studies show that the top 10% most popular videos in YouTube attract nearly 80% of total views [22]. In addition, it has been shown that with proper incentive and compensation mechanisms, users are willing to participate in D2D communications to reduce cost and donate resources to a P2P system for potential gains from it [23]–[25]. Given that the widely used smart personal devices are equipped with storage capabilities for file caching, in this paper, we devise a D2D-based P2P system, called Iunius to facilitate the local caching and harvesting of common files among UEs in a cellular network, where D2D communications utilise the UL radio resources. The ultimate goals are to significantly offload data traffic from the cellular BSs and core networks, and to reduce the overall system energy consumption.

The main contributions of this paper are summarised as follows. First, we propose a new D2D-based P2P protocol, which incorporates context information of physical-layer transmissions to improve user experiences. Second, in order to fully support the proposed P2P protocol, we present a new interference cancellation technique for UL CC receivers (i.e., BSs). Third, we enhance the greedy perimeter stateless routing (GPSR) scheme [26] with BS assistance to support multi-hop D2D communications over a large area. Finally, we propose an optimised RRM scheme to maximise the total throughput of D2D communications while guaranteeing the UL QoS requirements of CC UEs. This RRM scheme considers all the three aforementioned efforts and makes D2D communications better support the proposed P2P protocol. Note that, these four contributions have largely been studied separately before. In this paper, we design and optimise them jointly. Simulation results show that with this joint optimisation the Iunius system can increase UE throughput with less energy consumption as compared to CC communications. These results would be useful in designing incentives to encourage UEs to participate as local cache and transmitter/relay in D2D based P2P systems.

The remainder of this paper is organised as follows. In Section II, we introduce the network model and the Iunius system. Section III presents the application layer P2P protocol. In Section IV, we present the BS assisted GPSR scheme, interference cancellation technique for CC UL, and RRM for multi-hop D2D communications. In Section V, we evaluate the performance of Iunius through simulations. Finally, conclusions and possible future extensions are given in Section VI.

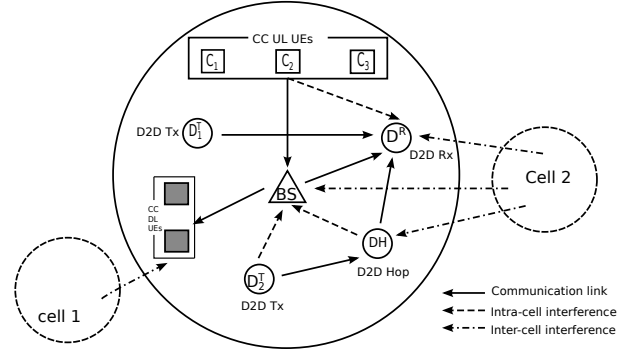


Figure 1. System model of P2P framework, where  $N_C^U = 3$  CC UL UEs and  $N_D^T = 2$  D2D links share the UL resources,  $N_C^D = 2$  CC DL UEs utilise the DL resources. The intra-cell interference includes the interference from D2D transmitters to the BS and the interference from the CC UEs to the D2D receivers. We also consider the inter-cell interference in our system model.

## II. IUNIUS SYSTEM AND NETWORK ARCHITECTURE

### A. Network Model

In this work, we consider a frequency division duplex (FDD) cellular system consisting of multiple cells, as depicted in Fig. 1. A BS equipped with an omni-directional antenna is deployed at the center of each cell. For BS assisted D2D communications, we assume that the inter-cell interference plus noise power can be estimated at the D2D receivers and the BSs [2]. The UL and DL channels each have a bandwidth of  $B$ , which is divided into  $K$  orthogonal subchannels. D2D communications may fully reuse the UL radio resources. A signal-to-interference-plus-noise ratio (SINR) of  $\Gamma_D$  is required for a reliable link to be established between a D2D transmitter and a D2D receiver.

There are three types of UEs: 1)  $N_C^D$  DL CC UEs; 2)  $N_C^U$  UL CC UEs; and 3)  $n$  D2D UEs in the coverage area of a BS. The CC UL and DL UEs are uniformly distributed in the network [14] and communicate with their serving BS directly. A pair of D2D UEs communicate with each other in an ad-hoc fashion over a single or multiple hops, bypassing the BS. We consider one D2D destination receiver  $d_R$ , which requires data from the set  $\mathcal{D}_T = \{d_1^T, \dots, d_{N_D}^T\}$  of  $N_D$  D2D sources. If there is no direct link available between a D2D source and the D2D destination, relays can be selected from the set  $\mathcal{D}_H = \{d_1^H, \dots, d_{N_H}^H\}$  of  $N_H$  idle D2D UEs (by the algorithm to be described in Section IV-A). The D2D relays are decode-and-forward half-duplex (DF-HD) relays [27]. Accordingly, the set of all D2D UEs is given by  $\mathcal{D} = \mathcal{D}_T \cup \mathcal{D}_H \cup \{d_R\}$  with the total number of D2D UEs  $n = N_D + N_H + 1$ . If the file or data requested by the D2D destination is not fully cached by the D2D sources, then the BS will transmit the rest of data through the CC DL.

The channel model consists of distance dependent path loss, fading and shadowing. Accordingly the channel gain  $g$  of a link is given by

$$g = \kappa d^{-\alpha} \|h\|^2 \zeta, \quad (1)$$

where  $\kappa$  is a constant determined by the environment [28],  $d$  is the distance between the transmitter and the receiver,  $\alpha$

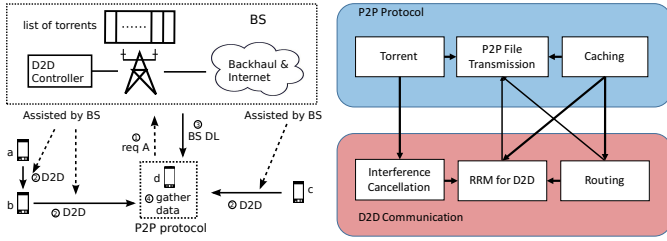


Figure 2. Iunius system model. The left part shows how Iunius works.  $a, b, c, d$  are four Iunius subscribers.  $d$  requests file  $A$  through P2P protocol.  $a$  and  $c$  are required by BS to transmit parts of file  $A$  to  $d$  via BS assisted D2D communications.  $b$  acts as the relay in the multi-hop D2D communications. Finally  $d$  gathers data from all links through P2P protocol. The right part shows how the core components in Iunius are interrelated to each other.

is the path loss distance exponent,  $h$  is the Rayleigh fading coefficient, and  $\zeta$  denotes the log-normal shadowing.

### B. Iunius System

Fig. 2 shows the Iunius system architecture, which consists of a spatially distributed cache system to provide local file caching services. Iunius subscribers, i.e., the UEs participating in the Iunius system, would cache a list of pre-selected files. Each of these files can be fully or partially cached in Iunius. How each file is divided into chunks and stored at different subscribers is described by a *torrent*. Each BS maintains a list of torrents and has full knowledge of the data stored in each Iunius subscriber associated with it. As we can see in Fig. 2, a subscriber can receive a locally cached file through the following four sub-routines:

- 1) **Request:** A Iunius subscriber requests a file through the P2P protocol from the BS.
- 2) **D2D:** The BS then requests proper Iunius subscribers to transfer the data to the requesting subscriber via BS assisted D2D communications, where the BS chooses the route from the D2D source to the D2D destination.
- 3) **BS DL:** For any partially, locally cached file or any failed end-to-end transmission, the BS transmits the remaining parts of the file to the requesting subscriber.
- 4) **Data gathering:** The requesting subscriber gathers the data from multiple D2D sources and the BS DL through the P2P protocol.

Note that Iunius subscribers would act as CC UEs when they either do not request any locally cached files or are not involved in D2D communications as sources or relays.

As shown in Fig. 2, the Iunius system consists of two major parts: an application layer P2P protocol and physical layer D2D communications. The components in Iunius are interrelated to each other as shown in Fig. 2. The torrent files (see Section III-A) and the local caching (see Section III-B) support the P2P file transmissions in application layer. The proposed context-aware P2P protocol enables the interference cancellation in Iunius (see Section IV-B). Then we propose an optimised RRM scheme (see Section IV-C) for D2D communications, considering the caching, routing and interference cancellation factors, and thereby better supporting the P2P file sharing.

## III. P2P PROTOCOL

In this section, we demonstrate our P2P protocol design from three key aspects: *torrent*, *spatially distributed caching system*, and *P2P file transmission*. The BS maintains and updates a list  $\mathcal{F}$  of pre-selected files for the Iunius system. Each file in  $\mathcal{F}$  is split into *chunks*, which are cached by a group of Iunius subscribers. The chunking and location information of a file is stored in a *torrent*. When a Iunius subscriber  $d_R$  requests a file  $F \in \mathcal{F}$  via the P2P protocol, the *P2P file transmission* would be set up by the system.

### A. Torrent

The BS maintains a list  $\mathcal{T}$  of torrents, each containing the following information:

- Identifier: Each torrent has a unique identifier and represents exactly one file [4].
- Application layer information: We adopt BitTorrent protocol [4] for the application layer P2P protocol, including both *metainfo* and *tracker* information of BitTorrent protocol. In addition, we add the location information of the peers, i.e., Iunius subscribers, to the *peer* part of BitTorrent protocol. Thus each Iunius subscriber is required to periodically report its location, which can be obtained by the Global Positioning System (GPS) that is available in most contemporary mobile devices.
- Cache information: 1) the identifier and content of each chunk; and 2) which Iunius subscriber each chunk is cached to.
- Context information: We adopt CA-P2P protocol [6] for the transmission of a chunk.

### B. Spatially Distributed Caching System

In the spatially distributed caching system, when a Iunius subscriber  $d_R$  receives data through the P2P protocol, it automatically caches the received data if it has available storage space. If it is out of storage space, then it will report to the BS. The BS will decide what data should be cached in  $d_R$  and return a series of instructions which would be executed by  $d_R$  to update its cache. The communications between the BS and  $d_R$  utilise the CC UL and DL links and the BS takes the following steps to make caching decisions:

- Step 1 Initialize four lists: the **CURRENT** list contains the identifiers of the chunks already cached at  $d_R$  according to  $\mathcal{T}$ ; the **ADD** list holds the identifiers of the newly received chunks at  $d_R$ ; the **ALL** list consists of both **CURRENT** and **ADD** lists; and the **REMOVE** list is initialised as an empty list.
- Step 2 Remove redundancy: remove all the identifiers of chunks that are already cached by other subscribers within a distance  $p$  to  $d_R$  from the lists **CURRENT**, **ADD** and **ALL**, and put the chunk identifiers removed from **CURRENT** into the list **REMOVE**.
- Step 3 Check storage availability: if all the chunks corresponding to **ALL** can be fully cached into  $d_R$ , the BS sends the (**ADD**, **REMOVE**) lists to  $d_R$  and  $d_R$  caches all the chunks of **ADD** and removes all

the chunks of **REMOVE**. The BS updates  $\mathcal{T}$  and terminates the decision process. Otherwise, move on to Step 4.

**Step 4** Classify the priority of chunks in **ALL**: among all chunks in the list **ALL**, the ones that have not been cached by any other subscribers are given the highest priority and with their identifiers put in the list **NEW**. The remaining chunks in **ALL** are classified into different **POPULARITY** groups according to the popularity of their relevant files. The popularity of a file can be defined according to the frequency or the most recent time of being requested. The priorities of the **POPULARITY** groups are ranked in descending order of their popularity.

**Step 5** Remove the lowest priority chunks: remove the identifiers of chunks of the lowest priority group from the lists **CURRENT**, **ADD** and **ALL**, and put the chunk identifiers removed from **CURRENT** into the list **REMOVE**. Go back to Step 3.

The above BS decision process achieves four goals: 1) *Spatially distributed caching with redundancy avoidance*: Step 3 enables every subscriber to cache the data they receive via the P2P protocol, and Step 2 eliminates the redundancy of a chunk being cached in several Iunius subscribers. 2) *Caching fairness*: the chunks that haven't been cached by any subscribers are given the highest priority, and would first be locally cached when there is storage available (Steps 4 and 5). 3) *Removal of Least Recently Used (LRU) chunks* [29]: Step 5 removes the chunks belonging to the LRU files from the spatially distributed caching system first. 4) *Efficiency*: It requires only two messages to be exchanged between the BS and the Iunius subscriber  $d_R$  to accomplish the whole BS decision process, i.e.,  $d_R$  uploads the **ADD** list to the BS and the BS sends back the (**ADD**, **REMOVE**) lists after the decision has been made. Moreover, each list contains only the identifiers of chunks and thus leads to a small size of each message. Therefore, the proposed mechanism ensures that only necessary information is exchanged between the BS and an Iunius subscriber and that the communication overhead is kept at minimum.

### C. P2P File Transmission

Each Iunius subscriber maintains a list of torrent identifiers. When subscriber  $d_R$  requests the file  $F(\in \mathcal{F})$  through the P2P protocol, the BS chooses a group of subscribers  $\mathcal{D}_T$  as source nodes to send chunks of  $F$  to  $d_R$  via D2D transmissions based on the following rules.

- **Uniqueness**: A chunk is transmitted by at most one subscriber in the group  $\mathcal{D}_T$ .
- **Proximity**: The BS first chooses the subscribers in the neighbourhood of the requesting subscriber  $d_R$  to transmit chunks of  $F$  to it. The neighbourhood of a subscriber is defined as the area in which a direct link between the subscriber and any other subscribers can be established following the mechanism to be presented in Section IV.
- **Isolation**: If some chunks of  $F$  are not cached in the neighbourhood of  $d_R$ , then the BS chooses the subscribers outside the neighbourhood of  $d_R$ . Since the

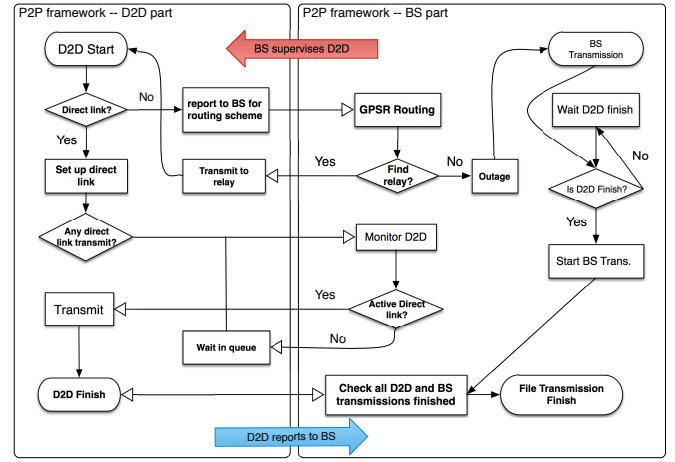


Figure 3. P2P framework flow chart. It shows the process of BS assisted D2D communications carrying out the proposed P2P protocol. The BS supervises the D2D transmissions and D2D pairs report to the BS of their state changes. BS also transmits all the chunks that cannot be transmitted by D2D communications to the receiver. The lines with solid arrows indicate the process within D2D part/BS part, and the lines with blank arrows denote the communications between D2D and the BS.

chunks cached by subscribers outside the neighbourhood of  $d_R$  would require multi-hop D2D transmissions to reach  $d_R$ , the selected subscribers are preferred to be far apart from each other so that they can transmit data simultaneously to different relays without causing significant interference.

- **Greediness**: Subscribers would be chosen into the group  $\mathcal{D}_T$  until: 1) no more subscribers can fulfil the *proximity* or *isolation* condition; or 2) no more subscribers have cached any chunks of  $F$  that have not been cached in  $\mathcal{D}_T$ .

The overall P2P file transmission mechanism is described by the flow chart in Fig. 3. We now devise a physical layer D2D communication scheme to handle the application layer P2P data transmission. At first, each D2D source in the selected group  $\mathcal{D}_T$  checks whether it can set up a reliable direct link (i.e.,  $\text{SINR} > \Gamma_D$ ) to the D2D destination. The infrastructure proposed in [6] and the method proposed in [30] can be used for two D2D UEs to know the link quality between them. When a direct link is not available, the BS assists the two D2D UEs to find a D2D relay utilising the GPSR algorithm (to be presented in Section IV-A). Outage might occur in two situations: 1) GPSR algorithm fails to find an idle Iunius subscriber as relay; or 2) the SINR at the selected relay is less than  $\Gamma_D$ . If outage occurs, the D2D transmitter reports outage to the BS, and the BS will transmit the corresponding data to the D2D destination via CC DL. These operations will repeat until all requested locally-cached chunks are received by the requesting subscriber  $d_R$ . The framework in [6] is used to update the BS on the transmission states of D2D communications in a real-time manner (see Section III-A). Thus, the BS can determine whether or not there exists any active direct D2D link, or identify a relay device for the D2D device to set up a new direct D2D link.

As required for DF-HD relay, there is only one active D2D link allowed at a time slot  $t$  for each multi-hop D2D route.

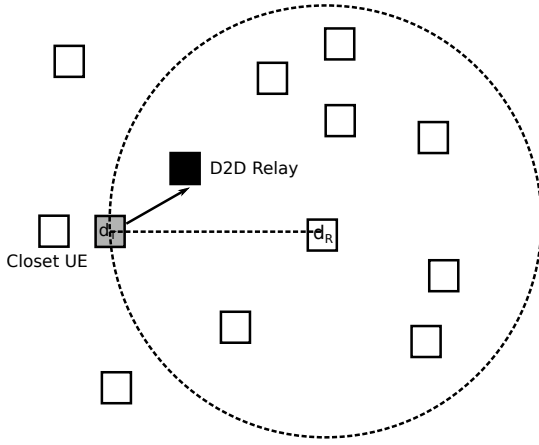


Figure 4. GPSR algorithm.  $d_T$  is the D2D transmitter and  $d_R$  is the target D2D receiver. The idle subscriber in black is chosen as the relay. The closest idle subscriber to the transmitter is not chosen as it is not in the circle area.

In addition, there is only one active direct link to  $d_R$  allowed during a time slot  $t$ . If there are more than one direct links to  $d_R$  waiting for transmission, the BS chooses the direct link with the best link quality to be active while withholding the others. The transmissions from different D2D transmitters to different relays would conduct simultaneously. The *isolation* characteristics of the D2D sources in  $\mathcal{D}_T$ , the GPSR algorithm (proposed in Section IV-A) and the RRM scheme (presented in Section IV-C) ensure that there will be no significant mutual interference between the concurrent D2D transmissions. Each active D2D link would utilise all the reliable UL subchannels. Finally, the BS would transfer any requested data that are not locally cached by the subscribers in  $\mathcal{D}_T$  to  $d_R$ .

#### IV. DEVICE-TO-DEVICE COMMUNICATIONS

In support of the D2D based P2P transmissions, in this section we develop a routing scheme and a joint resource allocation and power control scheme to maximize the throughput of D2D communications while maintaining the QoS of UL CC communications. Furthermore, we prove that in the Iunius system the interference from D2D communications to CC UL communications is negligible.

##### A. Greedy Perimeter Stateless Routing for D2D

For cases when there is no reliable direct link between a D2D source and the destination, we propose a multi-hop D2D routing scheme based on the GPSR algorithm [26]. In GPSR-like routing protocols, there are two kinds of package forwarding modes: greedy mode and perimeter mode, which are used to forward packets alternately. A packet is first forwarded greedily to the destination according to the geolocations of relays until the packet reaches a relay with no neighbour closer to the destination than itself (i.e., a concave node), then the packet is forwarded using the perimeter mode until the packet reaches a node closer to the destination than the concave node (i.e., a progress node) [26]. In our proposed routing algorithm, both geolocations and channel conditions of relays are considered in the greedy mode, and in perimeter

mode (i.e., a concave node is identified), the concave node reports the status to the BS and the BS would send the related packet to the D2D destination. This can improve the routing efficiency and reduce the outage probability of multi-hop D2D communications. The proposed D2D routing algorithm is summarised as follows:

- *greedy mode*: The D2D source is first set as the transmitter  $d_T$ . An idle Iunius subscriber fulfilling the following two conditions will be selected as a relay for the D2D communication between transmitter  $d_T$  and the file requesting destination  $d_R$ : 1) it locates within the circle centred at  $d_R$  with a radius of the distance between  $d_T$  and  $d_R$  (see Fig. 4); and 2) it is the closest idle Iunius subscriber to  $d_T$  in the circle (see Fig. 4). The closest idle subscriber to  $d_T$  is selected in order to guarantee the least outage probability of D2D communications for each hop and reduce the energy consumption of each D2D transmitter along the multi-hop D2D route. If such a relay is selected, then the selected relay is set as  $d_T$  and the above relay selection repeats until either no qualifying relay can be found or a complete route is formed from the D2D source to the destination  $d_R$ .
- *perimeter mode*: if for a given  $d_T$ , the greedy mode fails to find a relay, then that  $d_T$  reports to the BS. The BS stops the D2D transmission and forwards the corresponding data to  $d_R$ .

##### B. Interference Cancellation for CC UL

Without loss of generality, we assume that the set  $\mathcal{C}_i$  of subchannels are allocated to CC UE  $i$ , where  $i = 1, \dots, N_C^U$ ,  $\bigcup_{i=1}^{N_C^U} \mathcal{C}_i = \{1, \dots, K\}$ , and  $\mathcal{C}_i \cap \mathcal{C}_j = \emptyset$  for any  $i \neq j$ . Since the data to be transmitted and the modulation and coding scheme of the D2D transmissions are known by the BS (see *context info* in Section III-A), we have the following proposition for CC UE  $i$ .

**Proposition 1.** *The UL channel capacity  $T_i^c$  of CC UE  $i$  at subchannel  $c$  is given by*

$$T_i^c = \frac{B}{K} \log_2 \left( 1 + \frac{g_i^c P_i^c}{\sum_{m \in \mathcal{C}} I_i^m + N_0} \right), \quad (2)$$

where  $c \in \mathcal{C}_i$ ,  $\mathcal{C}$  is the set of cells in the neighbourhood,  $g_i^c$ ,  $P_i^c$  and  $I_i^m$  are the channel gain (as defined in (1)), the transmit power and the received power of the interference from cell  $m$  at subchannel  $c$  in the UL of CC UE  $i$ , respectively, and  $N_0$  is the additive white Gaussian noise (AWGN) power.

*Proof:* See Appendix. ■

Proposition 1 indicates that the interference from D2D communications to CC UL communications is cancelled in the Iunius system. As a result, the UL SINR of a CC UE and its throughput are not affected by D2D transmissions.

##### C. Radio Resource Management Scheme for D2D

In this subsection, we propose a RRM scheme to maximize the total throughput of D2D links subject to QoS requirements of UL CC UEs.

Consider the D2D source  $d_j^T (\in \mathcal{D}_T)$ , which requires  $n_j$  hops  $\mathcal{H}_j = \{h_1^j, \dots, h_{n_j}^j\}$  to reach the D2D destination. At

time slot  $t$ ,  $T_a^j$  is the data rate of the current hop  $h_a^j \in \mathcal{H}_j$ , in which the D2D transmitter is  $d_a^j$ . We have

$$T_a^j = \frac{B}{K} \sum_{k=1}^K \chi_{d_a^j}^k \log_2(1 + \gamma_{d_a^j}^k). \quad (3)$$

where  $\gamma_{d_a^j}^k$  is the receiver SINR of the hop  $h_a^j$  and is given by

$$\gamma_{d_a^j}^k = \frac{g_{d_a^j}^k P_{d_a^j}^k}{g_{i,d_a^j}^k P_i^k + Q_{d_a^j}^k + N_0} \quad (4)$$

where  $g_{d_a^j}^k$  and  $g_{i,d_a^j}^k$  are the channel gains (as defined in (1)) of the D2D link and the interfering link from CC UE  $i$  (which is transmitting at subchannel  $k$ ) to the D2D receiver, respectively,  $P_{d_a^j}^k$  and  $P_i^k$  are the transmit power of the D2D transmitter  $d_a^j$  and the CC UE  $i$  at the  $k^{\text{th}}$  subchannel, respectively,  $Q_{d_a^j}^k$  is the inter-cell interference power received by the D2D receiver at subchannel  $k$ , and the subchannel assignment indicator  $\chi_{d_a^j}^k$  is defined as

$$\chi_{d_a^j}^k = \begin{cases} 1, & \text{if subchannel } k \text{ is allocated to } d_a^j, \\ 0, & \text{otherwise.} \end{cases} \quad (5)$$

According to Section III-C, we assume in (3) that the mutual interference between any two simultaneously active D2D links is negligible.

At time slot  $t$  the D2D transmitters of all active D2D links form a group  $\mathcal{D}_A^t$ . The total throughput  $T_D^t$  of all active D2D links at time  $t$  is given by

$$T_D^t = \sum_{d_a^j \in \mathcal{D}_A^t} T_a^j. \quad (6)$$

We propose to maximise the total throughput of all active D2D links via joint resource allocation and power control as follows.

$$\text{OPT1: } \arg \max_{P_C, P_D, \chi_D} T_D^t \quad (7)$$

subject to

$$\sum_{c \in \mathcal{C}_i} T_i^c \geq \Phi_i, \quad i = 1, \dots, N_C^U, \quad (8)$$

$$0 \leq P_i^c \leq P_{\max}^C, \quad i = 1, \dots, N_C^U, \quad (9)$$

$$0 \leq P_{d_a^j}^k \leq P_{\max}^{d_a^j,k}, \quad \forall d_a^j \in \mathcal{D}_A^t, k = 1, \dots, K, \quad (10)$$

$$\gamma_{d_a^j}^k > \Gamma_D, \quad \forall d_a^j \in \mathcal{D}_A^t, k = 1, \dots, K, \quad (11)$$

$$\chi_{d_a^j}^k \in \{0, 1\}, \quad \forall d_a^j \in \mathcal{D}_A^t, k = 1, \dots, K. \quad (12)$$

where the  $K$ -by- $N_C^U$  matrix  $P_C$ , the  $K$ -by- $|\mathcal{D}_A^t|$  matrix  $P_D$  and the  $K$ -by- $|\mathcal{D}_A^t|$  matrix  $\chi_D$  contain transmit power for CC UL UEs, transmit power and subchannel assignment indicators for active D2D transmitters, respectively; if the  $k^{\text{th}}$  subchannel is not used by CC UE  $i$ , then the  $(k, i)^{\text{th}}$  element of  $P_C$  is 0;  $T_i^c$  is given in (2),  $\Phi_i$  is the minimum required UL data rate of CC UE  $i$ ,  $P_{\max}^C$  is the maximum transmit power per subchannel for a CC UE, and  $P_{\max}^{d_a^j,k}$  is the maximum D2D transmit power allowed in the  $k^{\text{th}}$  subchannel for the active D2D transmitter  $d_a^j$ . Constraint (8) guarantees the UL data rate requirements for CC UEs, where the data rate of CC UE

$i$  is the sum data rate of all subchannels allocated to it. To support the proposed P2P protocol, we define  $P_{\max}^{d_a^j,k}$  as

$$P_{\max}^{d_a^j,k} = \min \left\{ P_{\max}^C, \frac{P_\delta}{G_{d_a^j,k}^{d_a^j,k}} \right\}, \quad (13)$$

where  $P_\delta$  is a very low power level that is negligible by any D2D receiver,  $G_{d_a^j,k}^{d_a^j,k}$  is the largest channel gain in subchannel  $k$  of all the interfering links from  $d_a^j$  to the receivers of other active D2D links, and  $G_{d_a^j,k}^{d_a^j,k}$  can be estimated using the method in [14]. Thus  $P_{\max}^{d_a^j,k}$  is the maximum D2D transmit power that  $d_a^j$  can utilise without generating significant interference to other concurrent D2D transmissions. We use the statistical estimate of  $G_{d_a^j,k}^{d_a^j,k}$ , i.e.,  $\bar{G}_{d_a^j,k}^{d_a^j,k} = \mathbb{E}[G_{d_a^j,k}^{d_a^j,k}]$ , as discussed in [14]. Accordingly, the maximum transmit power for  $d_a^j$  at the  $k^{\text{th}}$  subchannel is given by  $P_{\max}^{d_a^j,k} = \min\{P_{\max}^C, P_\delta/\bar{G}_{d_a^j,k}^{d_a^j,k}\}$ .

To solve the joint optimisation problem in (7) directly would be difficult. From Proposition 1, we know that the D2D transmit power  $P_D$  will not affect the throughput of CC UEs. Following (13), the mutual interference between coexisting D2D links is negligible. Thus, for any given feasible  $P_C$ , the objective function in (7) is monotonically increasing with  $P_{d_a^j}^k$ . Therefore, the total throughput of all active D2D links is maximized by each D2D transmitter transmitting in all UL subchannels with the maximum allowed D2D transmit power, i.e., the optimal D2D transmit power and subchannel allocations are given by

$$\begin{cases} P_{d_a^j}^{k,*} = P_{\max}^{d_a^j,k} \\ \chi_{d_a^j}^{k,*} = 1 \end{cases}, \quad d_a^j \in \mathcal{D}_A^t, k = 1, \dots, K. \quad (14)$$

#### D. Power Control for CC UL UEs

Following (14), the optimisation problem (7) can be simplified as

$$\text{OPT2: } \arg \min_{P_C} -\frac{B}{K} \sum_{d_a^j \in \mathcal{D}_A^t} \sum_{k=1}^K \log_2 \left( 1 + \frac{g_{d_a^j}^k P_{\max}^{d_a^j,k}}{g_{i,d_a^j}^k P_i^k + Q_{d_a^j}^k + N_0} \right) \quad (15)$$

subject to

$$-\sum_{c \in \mathcal{C}_i} T_i^c \leq -\Phi_i, \quad i = 1, \dots, N_C^U \quad (16)$$

$$0 \leq P_i^c \leq P_{\max}^C, \quad \forall c \in \mathcal{C}_i, i = 1, \dots, N_C^U \quad (17)$$

It can be proven that the objective function in (15) is concave and the non-linear constraints (16) are convex. Hence, *OPT2* can be considered as a *global separable concave minimisation* problem [31], [32], and the widely used algorithm of [31] can be adopted to solve *OPT2*. Note that this is an *NP-hard* problem and the optimal solution can not be achieved in linear computational time. In the following we propose a reduced-complexity sub-optimal solution for *OPT2*.

We first discuss the necessary and sufficient conditions for *OPT2* to have a feasible solution. As the data rate  $T_i^c$  of CC UE  $i$  at the  $c^{\text{th}}$  subchannel is monotonically increasing with the transmit power  $P_i^c$ , the total data rate  $\sum_{c \in \mathcal{C}_i} T_i^c$  of CC UE

$i$  reaches its maximum value when  $P_i^c = P_{\max}^c, \forall c \in \mathcal{C}_i$ . We then have the following conclusion.

**Lemma 1.** *The necessary and sufficient condition for OPT2 is*

$$\Phi_i \leq \Phi_i^\dagger = \frac{B}{K} \sum_{c \in \mathcal{C}_i} \log_2 \left( 1 + \frac{g_i^c P_{\max}^c}{Q_i^c + N_0} \right). \quad (18)$$

*Proof:* The sufficiency can be proven by combining Proposition 1, (2) and (16). For an arbitrary  $\Phi_i \leq \Phi_i^\dagger$ , the solution  $x_0^i$  to the following equation exists [33], and apparently it satisfies (16).

$$\prod_{c \in \mathcal{C}_i} \left( 1 + \frac{g_i^c x_0^i}{Q_i^c + N_0} \right) = 2^{K\Phi_i/B}. \quad (19)$$

As  $T_i^c$  is monotonically increasing with  $P_i^c$ , we have  $x_0^i \leq P_{\max}^i$ . Thus  $x_0^i$  is a feasible solution of (15). The necessity is proven. ■

Hereafter, we assume that  $\Phi_i$  fulfils Lemma 1. Denote  $f(P_C)$  as the objective function in (15) and  $\mathbf{P}_i$  as the  $|\mathcal{C}_i|$ -by-1 vector of transmit power allocated to the subchannels utilised by the CC UE  $i$ . As each subchannel is assigned to at most one CC UE in each cellular cell,  $\mathbf{P}_i, \forall i = 1, \dots, N_C^U$ , are a sequence of disjoint sets. According to the definition of the sets  $\mathcal{C}_i$  in Section IV-B, we have  $f(P_C) = \sum_{i=1}^{N_C^U} f_i(\mathbf{P}_i)$ , where

$$f_i(\mathbf{P}_i) = -\frac{B}{K} \sum_{c \in \mathcal{C}_i} \sum_{d_a^j \in \mathcal{D}_A^i} \log_2 \left( 1 + \frac{g_{d_a^j}^c P_{\max}^{d_a^j, c}}{g_{i, d_a^j}^c P_i^c + Q_{d_a^j}^c + N_0} \right). \quad (20)$$

Thus, minimising the objective function  $f(P_C)$  is equivalent to minimising each  $f_i(\mathbf{P}_i)$ . Accordingly, OPT2 is transformed into OPT3 as follows,

$$\text{OPT3: } \arg \min_{\mathbf{P}_i} f_i(\mathbf{P}_i), \quad \forall i = 1, \dots, N_C^U \quad (21)$$

subject to

$$-\sum_{c \in \mathcal{C}_i} T_i^c \leq -\Phi_i, \quad i = 1, \dots, N_C^U, \quad (22)$$

$$0 \leq P_i^k \leq P_{\max}^C, \quad \forall k \in \mathcal{C}_i, i = 1, \dots, N_C^U. \quad (23)$$

We then construct an algorithm to solve each subproblem of OPT3. Denote

$$f_i^c(P_i^c) = -\sum_{d_a^j \in \mathcal{D}_A^i} \log_2 \left( 1 + \frac{g_{d_a^j}^c P_{\max}^{d_a^j, c}}{g_{i, d_a^j}^c P_i^c + Q_{d_a^j}^c + N_0} \right), \quad (24)$$

then  $f_i(\mathbf{P}_i) = -B/K \sum_{c \in \mathcal{C}_i} f_i^c(P_i^c)$ . It can be shown that  $f_i^c(P_i^c), c \in \mathcal{C}_i$ , are concave functions. This indicates that each subproblem of OPT3 can be transformed into a *global separable concave minimisation* problem [31].

**Definition 1.** *A rectangular domain is defined as  $\mathcal{R} = \{x_i | l_i \leq x_i \leq h_i, i = 1, \dots, n\}$ .*

**Definition 2.** *A set  $\tilde{\mathcal{R}}$  is a compact convex set iff*

- It is a compact set.
- For every  $x_1, x_2 \in \tilde{\mathcal{R}}$  and  $0 < \lambda < 1, \lambda \in \mathbb{R}$ , the point  $\lambda x_1 + (1 - \lambda)x_2 \in \tilde{\mathcal{R}}$ .

**Definition 3.** *For a continuous function  $f(x)$  defined on a compact convex set  $\tilde{\mathcal{R}}$ , a function  $\tilde{h}(x)$  is its convex envelope iff*

- $\tilde{h}$  is a convex function on  $\tilde{\mathcal{R}}$ .
- $\tilde{h}(x) \leq f(x)$  for every  $x \in \tilde{\mathcal{R}}$ .
- If  $h(x)$  is a convex function defined on  $\tilde{\mathcal{R}}$  such that  $h(x) \leq f(x)$  for all  $x \in \tilde{\mathcal{R}}$ , then  $\tilde{h}(x) \leq h(x)$  for all  $x \in \tilde{\mathcal{R}}$ .

**Theorem 1.** *The convex envelope  $\tilde{h}(x)$  for a separable concave function  $f(x) = \sum f_i(x_i), i = 1, \dots, s$ , defined on a set  $\tilde{\mathcal{R}} \cap \mathcal{R}$ , where  $\tilde{\mathcal{R}}$  is a compact convex set and  $\mathcal{R} = \{x_i | l_i \leq x_i \leq h_i, i = 1, \dots, n\}$  is a rectangular domain, is given by*

$$\tilde{h}(x) = \sum_{i=1}^s (a_i x_i + b_i), \quad (25)$$

where  $a_i$  and  $b_i$  are defined as

$$a_i l_i + b_i = f_i(l_i), \quad a_i h_i + b_i = f_i(h_i) \quad (26)$$

*Proof:* See [31], [32]. ■

**Corollary 1.** *For the optimisation problem defined in OPT3, denote  $\tilde{h}_{v,i}(\mathbf{P}_i)$  as the convex envelope of  $f_i(\mathbf{P}_i)$  on any rectangular domain  $\mathcal{R}_{v,i} = \{P_i^c | l_{v,i}^c \leq P_i^c \leq h_{v,i}^c, c \in \mathcal{C}_i\} \subseteq \mathcal{R}_{0,i}$ , where  $\mathcal{R}_{0,i}$  is the feasible rectangular domain of (23), then we have*

$$\tilde{h}_{v,i}(\mathbf{P}_i) = \sum_{c \in \mathcal{C}_i} (a_{v,i}^c P_i^c + b_{v,i}^c), \quad (27)$$

where  $a_{v,i}^c$  and  $b_{v,i}^c$  are given by

$$\begin{bmatrix} a_{v,i}^c \\ b_{v,i}^c \end{bmatrix} = \begin{bmatrix} l_{v,i}^c & 1 \\ h_{v,i}^c & 1 \end{bmatrix}^{-1} \begin{bmatrix} f_i^c(l_{v,i}^c) \\ f_i^c(h_{v,i}^c) \end{bmatrix} \quad (28)$$

*Proof:* We prove that the feasible domain of (22),  $\tilde{\mathcal{R}}_i$ , is a compact convex set. First, we have  $\tilde{\mathcal{R}}_i \subset \mathcal{R}_{0,i}$ , thus  $\tilde{\mathcal{R}}_i$  is bounded and closed, i.e.,  $\tilde{\mathcal{R}}_i$  is a compact set. As aforementioned,  $T_i^c$  is monotonically increasing with  $P_i^c$ , thus  $\tilde{\mathcal{R}}_i$  is also a convex set. According to Definition 1,  $\tilde{\mathcal{R}}_i$  is a compact convex set.

Note that (28) is the solution of (26). Then with Theorem 1, we prove this corollary. ■

Following the above discussion, we propose a power control algorithm in Fig. 5 to solve OPT3 based on the *branch-and-bound* algorithm [31]. In Fig. 5, we define two operators  $\ominus$  and  $\oplus$  (Lines 24–26) as removing a specific bound and adding a specific bound to a rectangular area, respectively. We use  $\{\cdot\}$  to represent the “array” concept in programming, which is a set of unordered elements. The power control algorithm initialises the vector  $\mathbf{R}$  with its only element given by  $\mathcal{R}_{0,i}$  and the index of iteration  $q$  as 1.

In the  $q^{\text{th}}$  iteration,  $\mathcal{R}_{0,i}$  is subdivided into  $s_q$  rectangular domains, which are put into the vector  $\mathbf{R}$  (Lines 4–6). For each rectangle  $\mathcal{R}_{v,i}$  (Line 6), the algorithm calculates the convex envelope function  $\tilde{h}_{v,i}(\mathbf{P}_i)$  defined in (27) and (28) (Lines 7–9,13) and the associated solution  $\mathbf{P}_C^v$  of the convex optimisation problem defined as follows (Lines 14,15).

$$\text{OPT4: } \arg \min_{\mathbf{P}_i} \tilde{h}_{v,i}(\mathbf{P}_i) \quad (29)$$

$$\text{subject to } \mathbf{P}_i \in \tilde{\mathcal{R}}_i \cap \mathcal{R}_{v,i}$$

```

1: function CCPOWERCONTROL( $P_C^{\max}, \tilde{\mathcal{R}}_i, \mathcal{R}_{0,i}, \mathcal{C}_i, i$ )
2:   Initialise  $q \leftarrow 1; \mathbf{R} \leftarrow \{\mathcal{R}_{0,i}\};$ 
3:   repeat
4:      $\mathbf{P} \leftarrow \{\}; s_q \leftarrow \text{LEN}(\mathbf{R});$ 
5:     for all  $v = 1, \dots, s_q$  do
6:        $\mathcal{R}_{v,i} \leftarrow \mathbf{R}[v];$ 
7:       for all  $k \in \mathcal{C}_i$  do
8:          $(a_{v,i}^c, b_{v,i}^c) \leftarrow (28)$  with  $\mathcal{R}_{v,i};$ 
9:       end for
10:      if  $\mathcal{R}_i \cap \mathcal{R}_{v,i} = \emptyset$  then
11:         $P_C^v \leftarrow \emptyset; \mathbf{R} \leftarrow \mathbf{R} \ominus \mathcal{R}_{v,i};$ 
12:      else
13:         $\hat{h}_{v,i}(\cdot) \leftarrow (27)$  with  $(a_{v,i}^c, b_{v,i}^c);$ 
14:         $P_C^v \leftarrow \text{solve (29)}$  with  $\hat{h}_{v,i}(\cdot), \mathcal{R}_{v,i}$  and  $\tilde{\mathcal{R}}_i;$ 
15:         $\mathbf{P} \leftarrow \mathbf{P} \oplus P_C^v;$ 
16:      end if
17:    end for
18:     $s_q \leftarrow \text{LEN}(\mathbf{R});$ 
19:     $t \leftarrow \arg \min_v \hat{h}_{v,i}(P_C^v), \forall v = 1, \dots, s_q;$ 
20:     $\mathbf{P}_q^* \leftarrow \hat{\mathbf{P}}[t]; \hat{h}_{q,i}(\cdot) \leftarrow \sum_{c \in \mathcal{C}_i} \hat{h}_{i,i}^c(\cdot);$ 
21:     $r \leftarrow \arg \max_c (f_c(\mathbf{P}_q^*[c]) - \hat{h}_{i,i}^c(\mathbf{P}_q^*[c])), \forall c \in \mathcal{C}_i;$ 
22:     $\mathbf{P}_q^{*,r} \leftarrow \mathbf{P}_q^*[r];$ 
23:     $\mathcal{R}_q^l \leftarrow \mathcal{R}_{t,i} \ominus \{P_i^r | l_{t,i}^r \leq P_i^r \leq h_{t,i}^r\} \oplus \{P_i^r | l_{t,i}^r \leq P_i^r \leq P_q^{*,r}\};$ 
24:     $\mathcal{R}_q^u \leftarrow \mathcal{R}_{t,i} \ominus \{P_i^r | l_{t,i}^r \leq P_i^r \leq h_{t,i}^r\} \oplus \{P_i^r | P_q^{*,r} \leq P_i^r \leq h_{t,i}^r\};$ 
25:     $\mathbf{R} \leftarrow \mathbf{R} \ominus \mathcal{R}_{t,i} \oplus \mathcal{R}_q^l \oplus \mathcal{R}_q^u$ 
26:     $q \leftarrow q + 1$ 
27:    until  $f(\mathbf{P}_q^*) = \hat{h}_{q,i}(\mathbf{P}_q^*)$ 
28:    return  $\mathbf{P}_q^*$  as the solution to the  $i^{\text{th}}$  subproblem;
29: end function

```

Figure 5. Power control algorithm.

We notice that the intersection of  $\tilde{\mathcal{R}}_i$  and  $\mathcal{R}_{v,i}$  might be empty. In this case, we remove the rectangle  $\mathcal{R}_{v,i}$  from  $\mathbf{R}$  and continue the calculation for the next rectangle (Line 10–11). We choose the solution  $P_C^t$  of *OPT4* on the rectangle domain  $\mathcal{R}_{t,i}$ , which has the smallest objective function value (Line 19). Let  $\mathbf{P}_q^*$  denote  $P_C^t$  (Line 20). The algorithm terminates when  $f(\mathbf{P}_q^*) = \hat{h}_{q,i}(\mathbf{P}_q^*)$  (Line 27), and the solution  $\mathbf{P}_q^*$  is returned (Line 28). Otherwise, the weak branching rule is applied to divide the rectangle  $\mathcal{R}_{t,i}$  into two sub-rectangles as follows [32]: we first find the point  $r$  in  $\mathbf{P}_q^*$ , which maximises the difference between  $f_c(\mathbf{P}_q^*[c])$  and  $\hat{h}_{i,i}^c(\mathbf{P}_q^*[c]), \forall c \in \mathcal{C}_i$ ; we then divide  $\mathcal{R}_{t,i}$  into two rectangles at the point  $\mathbf{P}_q^*[r]$  (Lines 21–24). These two new rectangles replace the original  $\mathcal{R}_{t,i}$  in  $\mathbf{R}$  (Line 25). The above process repeats until the termination rule is fulfilled.

According to [34], any limit point generated by the proposed algorithm is a solution to a subproblem of *OPT3*. Therefore, we can relax the termination rule for the proposed algorithm as: when the iteration index  $q$  reaches a pre-determined maximum value, the algorithm terminates and returns the solution  $\mathbf{P}_q^*$ .

Finally we discuss a sub-optimal solution specifically tailored for current LTE/LTE-A systems, which use SC-FDMA in the UL. SC-FDMA requires an equal power allocation in all subchannels assigned to a UE to achieve a low peak-to-average power ratio. Thus the sub-optimal solution to *OPT2* can be obtained by solving the following equations for  $P_i^*$ ,

$$\prod_{c \in \mathcal{C}_i} \left( 1 + \frac{g_i^c P_i^*}{Q_i^c + N_0} \right) = 2^{K\Phi_i/B}, \quad i = 1, \dots, N_C^U. \quad (30)$$

Each equation in (30) is a polynomial of  $P_i^*$ . Thus it has

Table I  
SIMULATION PARAMETERS

Parameter	Value
Inter-site distance	500m
AWGN power density ( $N_0$ )	-120 dBm/Hz
Bandwidth	10 MHz
Frequency	2.3 GHz
Number of Subchannels	50
Pathloss exponent ( $\alpha$ )	2, 2.5, 3, 3.5, 4, 4.5
Distance threshold ( $\delta_d$ )	20m
Negligible power level ( $P_{\delta_D}$ )	-60 dBm
Number of CC UL UEs ( $N_C^U$ )	5
Number of CC DL UEs ( $N_C^D$ )	10
SINR threshold ( $\Gamma_D$ )	8.75 dB
Maximum transmit power $P_C^{\max}$	23 dBm
Multipath fading (Rayleigh distribution)	Scale parameter 0.5
Shadowing (Log-normal)	Standard deviation of 4 dB

a radical-expression solution when the highest order of the equation is less than five [33]. Otherwise, it can be solved using *Newton-Raphson* method numerically [33]. The matrix  $\mathbf{P}_C$  can be initialised as an all-zero matrix. It is worth noticing that the rate of convergence of *Newton-Raphson* method is high and several methods have been proposed to further improve the convergence rate [33].

In summary, the power control for the CC UL UEs and the RRM for the D2D communications can be performed as follows:

- Each D2D link is assigned with all available UL subchannels.
- Each D2D transmitter utilises the maximum allowed transmit power defined in (13) to ensure no significant mutual interference between D2D links.
- The transmit power of a CC UE follows the optimal power control algorithm presented in Fig. 5 or the sub-optimal solution defined in (30) for SC-FDMA UL in LTE/LTE-A systems.

## V. SIMULATION RESULTS

We perform Monte-Carlo simulation to evaluate the performance of Iunius. The simulation model consists of 19 hexagonal cells and each cell has 3 sectors as described in [28]. We use the channel model in Table B.1.2.1–1 (Urban Micro) in [28]. The remain important simulation parameters are summarised in Table I. The data rate threshold  $\Phi_i, \forall i = 1, \dots, N_C^U$  is randomly generated under the restriction defined in (18) (Lemma 1).

Fig. 6 plots the central cell where the Iunius system is deployed and evaluated. We randomly choose a position in the central cell as the location of the Iunius receiver. The Iunius subscribers are uniformly distributed in the central cell. The Iunius transmitters are chosen by rules described in the proposed P2P protocol. In Fig. 6, the circular area around the Iunius receiver is its neighbourhood area. In addition, the CC UL UEs and the CC DL UEs are generated following a spatial uniform distribution. Although we focus on the performance of the central cell, all the effects of neighbouring cells are included.

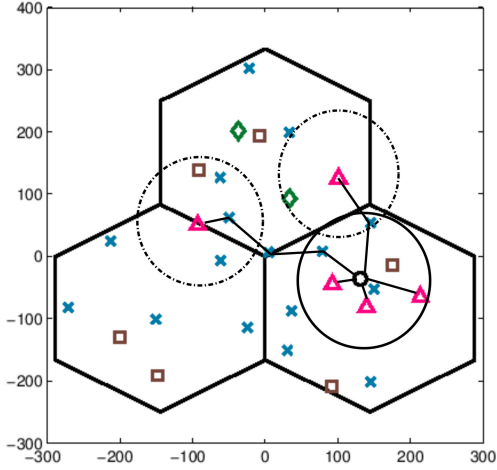


Figure 6. Simulation model. The figure shows the central cell while the 18 outer cells are omitted for simplicity. The chosen D2D transmitters (triangle shape) follow the *proximity* and *isolation* rules described in Section III-C. The red triangle, black circle, blue cross, green diamond and brown square represent the Iunius transmitters, Iunius receiver, idle Iunius subscribers, CC UL UEs and CC DL UEs, respectively.

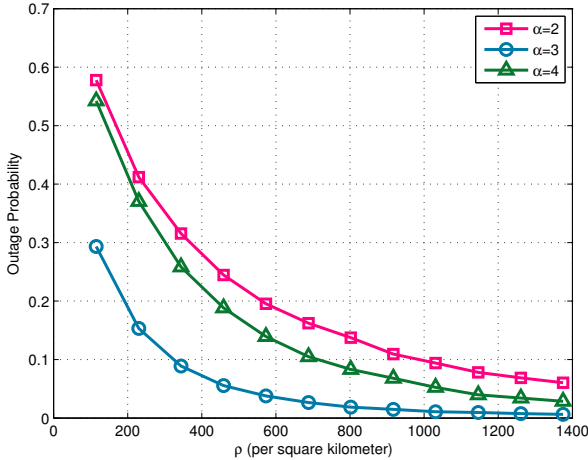


Figure 7. Simulated outage probability of D2D transmissions.

#### A. Outage Probability and Average Number of Hops

We first evaluate the outage probability and the average number of hops of the multi-hop D2D transmissions in the Iunius system. The outage probability is the probability of an outage event (as defined in Section III-C) occurring. These two metrics show the performance of the P2P protocol and the GPSR algorithm.

Assuming that the Iunius subscribers are uniformly distributed in the cellular network with a spatial density  $\rho$  (the number of Iunius subscribers per square kilometre), we show in Fig. 7 the outage probability of D2D transmissions versus the Iunius subscriber density  $\rho$ . We can see that for all path loss exponents considered the outage probability of D2D transmissions decreases as  $\rho$  increases. This is because with a higher density of Iunius subscribers, it is more likely for the

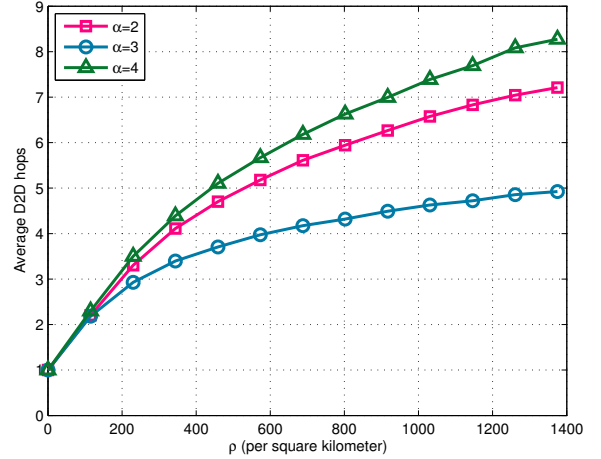


Figure 8. The average number of hops of D2D communications in the Iunius system versus the density of Iunius subscribers.

proposed P2P protocol and GPSR algorithm to find relays and the average transmission distance of each hop becomes shorter, thus reducing the outage probability. For each considered  $\alpha$ , when  $\rho$  gets larger than 1000, the outage probability falls below 0.1. This indicates that in high population density areas, such as city centres, our proposed P2P protocol and GPSR algorithm can efficiently find routes from D2D transmitters to the D2D destination, and thus can efficiently support the end-to-end data transmissions in the Iunius system.

Fig. 8 illustrates the average number of hops for D2D communications in the Iunius system versus the subscriber density  $\rho$ . We can see that for each considered  $\alpha$ , the average number of hops for D2D communications increases with  $\rho$ , while the rate of increase slows down at higher values of  $\rho$ . We note that for  $\alpha = 3$  even with a very high density of Iunius subscribers ( $\rho = 1400$ ), the average number of D2D hops is below 5. This ensures that the BS assisted D2D communications in the Iunius system would not overwhelm the BS.

From both Fig. 7 and Fig. 8 we note that, for a given  $\rho$ , the Iunius system achieves the lowest outage probability and requires the lowest average number of D2D hops in the moderate path loss environment ( $\alpha = 3$ ). According to (13) and (14) in Section IV-C, all the D2D communications utilise their maximum allowed transmit power  $P_{\max}^{d_a^j, k}$ . In a small path loss environment (e.g.,  $\alpha = 2$ ), the D2D communications are restricted to a small  $P_{\max}^{d_a^j, k}$  ( $P_{\max}^{d_a^j, k} \leq P_{\delta} / G_{d_a^j, k}$ ) and might suffer from severe interference from CC UL UEs, thus it has a larger outage probability and shorter transmission distance leading to more hops compared to those in the moderate path loss environment. On the other hand, in a large path loss environment ( $\alpha = 4$ ), the transmit power of D2D transmitters would not be significantly larger than that in the moderate path loss environment (as  $P_{\max}^{d_a^j, k} \leq P_{\max}^C$ ) while the D2D UEs are more isolated from each other, thus both the outage probability and the average number of hops are larger than those for  $\alpha = 3$ .

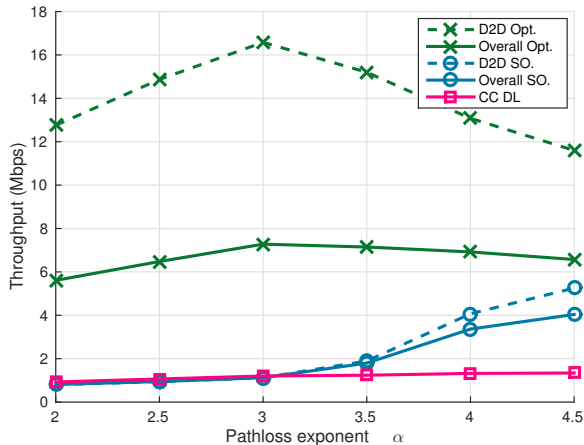


Figure 9. Throughput of D2D communications, the overall Iunius system, and CC DL versus path loss exponents (with file sharing ratio 90%).

### B. Throughput

Fig. 9 plots the throughput of D2D communications  $T_{DL}$ , the overall throughput of the Iunius system  $T_{Iunius}$  and the throughput of CC DL transmissions  $T_{D2D}$  versus the path loss exponent  $\alpha$ , where performance corresponding to both the proposed optimal RRM and sub-optimal RRM schemes is included,  $\rho = 700$ , and 90% of the requested file has been evenly cached by the randomly chosen D2D transmitters. The overall throughput of the Iunius system is calculated as

$$T_{Iunius} = \frac{1}{0.1/T_{DL} + 0.9/T_{D2D}}. \quad (31)$$

It can be seen that the D2D communications with the optimal RRM scheme achieves a much high throughput than that with the suboptimal RRM scheme in all path loss environments, so does the overall throughput of the Iunius system. In accordance with the results in Fig. 7 and Fig. 8, the throughput of the D2D communications with optimal RRM reaches its maximum (almost 17 Mbps) at  $\alpha = 3$ . As we can see from  $OPT2$  defined in (15) and its constraint (16), with the optimal RRM scheme and  $\rho = 700$ , the throughput of D2D communications scales with the transmit power  $P_{max}^{d_j,k}$  in (13), which increases with  $\alpha$  in small and moderate path loss environments but is capped by  $P_{max}^C$  in a high path loss environment where D2D UEs are isolated from each other, leading to the decrease of D2D throughput. With the sub-optimal RRM, the D2D throughput increases with  $\alpha$ . This is because the power control for CC UL UEs defined in (30) does not prevent the interference from CC UL UEs to the D2D communications and in a larger path loss environment the D2D communications are more isolated from the CC UL communications, i.e., suffer less interference from CC UL UEs. The overall throughput of the Iunius system with the optimal RRM is much higher than that of CC DL in all path loss environments, and the overall throughput with the suboptimal RRM is increasingly higher than the CC DL throughput at higher values of  $\alpha$ . This shows that the Iunius system significantly outperforms the CC system in terms of DL throughput.

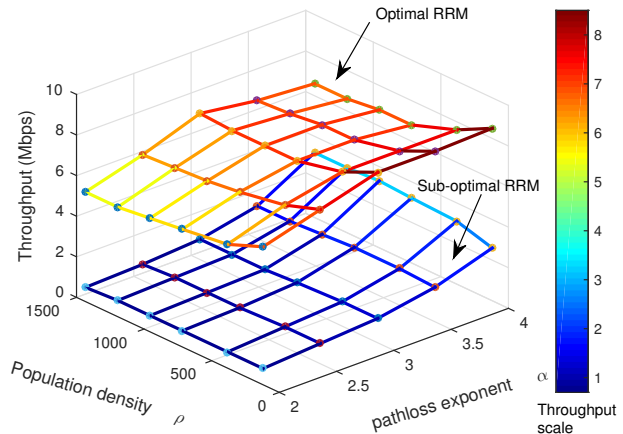


Figure 10. Iunius system throughput performance for different Iunius subscribers density  $\rho$  and path loss exponent  $\alpha$ . Different colors represent different throughputs of the Iunius system.

Fig. 10 compares the overall throughput of the Iunius system deploying the optimal and sub-optimal RRM schemes. For each considered pair of  $\rho$  and  $\alpha$ , the throughput achieved by the optimal RRM is much higher than that of the suboptimal RRM, with the gap between them decreasing with both  $\rho$  and  $\alpha$ . For the optimal RRM scheme, we can see that for a given  $\alpha$  the throughput of the Iunius system decreases with  $\rho$ , indicating that a high density of Iunius subscribers does not help to improve the performance of Iunius system deploying optimal RRM. This is mainly because with a higher  $\rho$ , more hops might be taken from the D2D source to the destination (see Fig. 8), thereby reducing the throughput. For a low density of Iunius subscribers ( $\rho < 500$ ), the throughput increases with  $\alpha$ . This is because with a lower  $\rho$ , the D2D transmissions have a longer average distance per hop and become more vulnerable to the interference from CC UL UEs, thus preferring a more isolated transmission environment (i.e., larger  $\alpha$ ). For the sub-optimal RRM scheme, we observe that the throughput always increases with  $\alpha$  for a given  $\rho$ . In small and moderate path loss environments ( $2 \leq \alpha \leq 3$ ), the throughput almost remains constant for different  $\rho$ . While in a high path loss environment ( $\alpha = 4$ ), the throughput increases with  $\rho$ . This shows that the sub-optimal RRM scheme is more applicable in a high path loss environment with a high Iunius subscriber density.

Fig. 11 illustrates the time consumptions of BS transmissions and D2D transmissions in the Iunius system deploying the optimal or sub-optimal RRM scheme versus the portion of file being locally cached in Iunius, which is denoted by the local cache portion  $\beta$ , for  $\rho = 700$ ,  $\alpha = 2, 3, 4$ . We can see that for given  $\beta$  and  $\alpha$ , the total time consumption with the optimal RRM scheme is much less than that with the suboptimal scheme, and the difference between the two schemes increases with  $\beta$  for a given  $\alpha$ . For a given  $\beta$ , the total time consumption, time for D2D transmissions, and time for BS transmissions all decrease with  $\alpha$  for both the optimal and suboptimal RRM schemes. For any  $\beta < 1$ , the time for BS transmissions always dominates the time consumption with the optimal RRM scheme. This is mainly due to the high

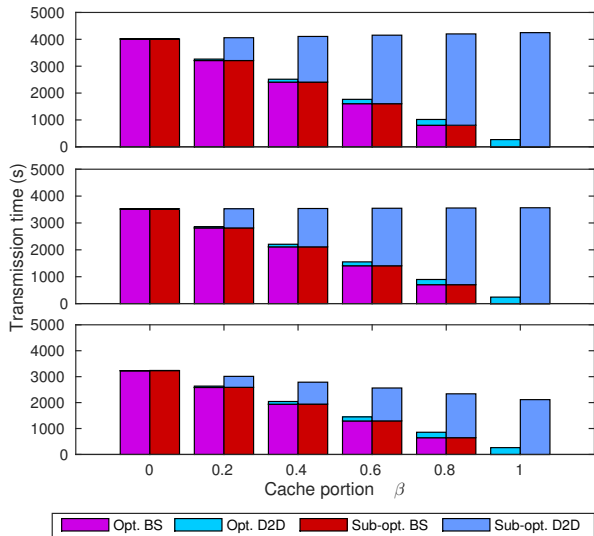


Figure 11. Transmission times in the Iunius system. From top to bottom,  $\alpha$  is 2, 3, 4, respectively.

throughput that D2D communications can achieve with the optimal RRM scheme. On the contrary, with the sub-optimal RRM scheme, when  $\beta > 0.6$  the time for D2D transmissions becomes dominant in the Iunius system. We note that, the total transmission time of the Iunius system will never exceed the time required by the CC DL solely ( $\beta = 0$ ) to transmit the same amount of data for any given  $\beta$  and  $\alpha$ . Thus, the Iunius system can efficiently offload traffic from the cellular BSs.

### C. Energy Saving

In the Iunius system, the total energy consumption of a multi-hop D2D route is determined by two parts: the number of hops from D2D source to its associated destination and the energy consumption for each hop, which is discussed in Section IV.

We quantify the energy saving of the Iunius system compared to the CC transmission versus the local cache portion  $\beta$  under the same setting as for Fig. 7 and Fig. 8. The normalised energy saving is defined as

$$E_{\text{save}} = \frac{E_{\text{BS}} - E_{\text{Iunius}}}{E_{\text{BS}}} \times 100\% \\ = \frac{E_{\text{BS}} - (\sum_{n=1}^{n_j} E_{\text{hop}}^n + E'_{\text{BS}})}{E_{\text{BS}}} \times 100\%, \quad (32)$$

where  $E_{\text{BS}}$  is the total energy consumed by the CC DL to transmit a data file of 4 Gbits at the data rate of 1 Mbps,  $E_{\text{Iunius}}$  is the total energy consumed by the Iunius system to deliver the same file at the same data rate,  $E_{\text{hop}}^n$  is the energy consumed by each D2D hop,  $n_j$  is the average number of D2D hops, and  $E'_{\text{BS}}$  is the energy consumed by the BS for transmitting the part of the file not locally cached in Iunius. We can see that with the same  $\beta$  and  $\alpha$ , the optimal RRM scheme achieves a higher energy saving than the suboptimal RRM scheme. For

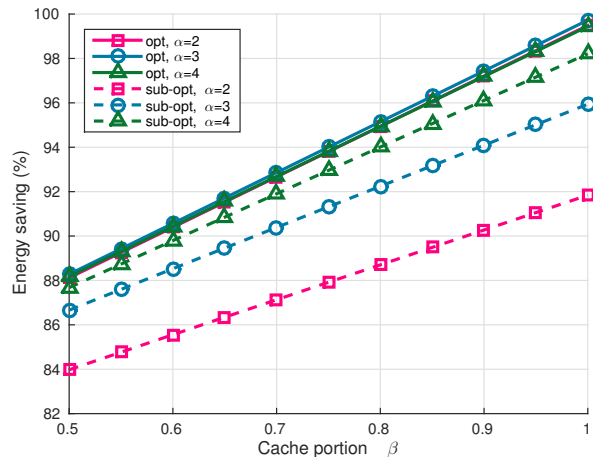


Figure 12. Energy saving of the Iunius system as compared to the CC system for transmitting the same amount of data.

a given  $\alpha$ , the energy saving of the Iunius system increases with  $\beta$  for both the optimal and suboptimal RRM schemes. With the optimal RRM scheme, for any given  $\beta$ , there is no significant difference in energy saving in different path loss environments. With the sub-optimal RRM scheme, that for a given  $\beta$  the energy saving increases with  $\alpha$ , and when  $\alpha = 4$  it achieves a similar energy saving as the optimal RRM. This is because the sub-optimal RRM scheme achieves a higher data rate for larger  $\alpha$  (as shown in Fig. 10), leading to a higher energy saving per hop. This surpasses the negative effect of a large number of D2D hops in a high path loss environment to energy saving.

### D. Computational Complexity

The superior performance of the proposed optimal RRM scheme over the sub-optimal RRM scheme is achieved at the cost of a very high computational complexity. In our simulations, the optimal RRM scheme has to solve more than 1000 convex optimisation problems defined in (29), while the sub-optimal RRM scheme can solve the problem in (30) within 20 loops.

## VI. CONCLUSION

In this paper we have proposed a novel peer-to-peer system based on D2D communications, called Iunius. The proposed P2P protocol combines the conventional application-layer P2P protocol and the routing and scheduling schemes in lower layers. An interference cancellation technique for the CC UL, a GPSR based routing algorithm for multi-hop D2D communications, and a semi-distributed RRM scheme for both CC UL and D2D communications have been proposed for D2D communications to support the proposed P2P protocol.

Simulation results have shown that the Iunius system significantly improves the network performance in terms of throughput, BS traffic offload and energy saving. The P2P protocol and the GPSR algorithm can efficiently find a route from the D2D source to the destination while keeping the outage probability

low. With the proposed interference cancellation technique, the Iunius system also guarantees the QoS of CC UL UEs.

To further improve the performance of the Iunius system, more cooperation between D2D links and other QoS requirements (such as error rate) for CC UEs could be considered. Mode selection between the proposed D2D-based P2P communications and the conventional directly downloading for the BS is another important research topic. Advanced network coding and cooperative communication techniques, can be applied to further enhance the system throughput and reduce the transmission delay. A more sophisticated local caching mechanism in conjunction with multi-hop routing for the Iunius system could also be an interesting topic of future work.

#### APPENDIX

We model the UL channel between CC UE  $i$  and the BS as a channel with state. We denote the output at BS as  $Y \sim f(y)$ , the signal from CC UE  $i$  and the inter-cell interference as input  $X \sim f(x)$ , and the signal from the interfering D2D link as the state  $S \sim f(s)$ . The channel can be expressed as

$$Y = X + S + N \quad (33)$$

where  $N \sim N(0, \sigma^2)$  denotes the Gaussian noise. From the theory proposed in [35], the channel capacity  $T_i^c$  can be expressed as

$$T_i^c = \max_{f(x)} I(X; Y, S) = \max_{f(x)} I(X; Y|S) \quad (34)$$

where  $I(X; Y|S)$  is the conditional mutual information. Denote the differential entropy as  $H(\cdot)$ , we have the following Lemma for the conditional entropy.

**Lemma 2.** *Given input  $X \sim f(x)$  and state  $S \sim f(s)$ , which are independent, for an output  $Y = X + S$ , we have  $H(Y|S) = H(X|S)$ .*

*Proof:*

$$\begin{aligned} H(Y|S) &= \int H(Y|S=s)f(s) ds \\ &= -\int f(s) \int f_{Y|S=s}(y|S=s) \log f_{Y|S=s}(y|S=s) dy ds \\ &= -\int f(s) \int f_{Y|S=s}(x+s|S=s) \log f_{Y|S=s}(x+s|S=s) d(x+s) ds \\ &= -\int f(s) \int f_{X|S=s}(x|S=s) \log f_{X|S=s}(x|S=s) dx ds \\ &= H(X|S) \end{aligned} \quad (35)$$

We assume  $X, S, N$  are independent. As discussed in Section II, the channel state information is available at the decoder. With Lemma 2, we have the following conclusion

$$\begin{aligned} I(X; Y|S) &= H(Y|S) - H(Y|X, S) \\ &= H(X + S + N|S) - H(X + S + N|X, S) \\ &= H(X + N|S) - H(N) \\ &= H(X + N) - H(N) \end{aligned} \quad (36)$$

According to the theory in [35], and considering the channel capacity in *bit/s*, we have

$$T_i^c = \max_{f(x)} I(X; Y|S) = \max_{f(x)} H(X + N) - H(N) = \frac{B}{K} \log_2 \left( 1 + \frac{g_i^c P_i^c}{Q_i^c + N_0} \right) \quad (37)$$

#### REFERENCES

- [1] K. Doppler, M. Rinne, C. Wijting, C. Ribeiro, and K. Hugl, "Device-to-device communication as an underlay to lte-advanced networks," *IEEE Communications Magazine*, vol. 47, no. 12, pp. 42–49, 2009.
- [2] G. Fodor, E. Dahlman, G. Mildh, S. Parkvall, N. Reider, G. Miklos, and Z. Turanyi, "Design aspects of network assisted device-to-device communications," *IEEE Commun. Mag.*, vol. 50, no. 3, pp. 170–177, 2012.
- [3] L. Wei, R. Hu, Y. Qian, and G. Wu, "Enable device-to-device communications underlying cellular networks: challenges and research aspects," *IEEE Commun. Mag.*, vol. 52, no. 6, pp. 90–96, June 2014.
- [4] A. Legout, G. Urvoy-Keller, and P. Michiardi, "Rarest first and choke algorithms are enough," in *Proceedings of the 6th ACM SIGCOMM Conference on Internet Measurement*, 2006.
- [5] I. Stoica, R. Morris, D. Liben-Nowell, D. R. Karger, M. F. Kaashoek, F. Dabek, and H. Balakrishnan, "Chord: A scalable peer-to-peer lookup protocol for internet applications," *IEEE/ACM Trans. Netw.*, vol. 11, no. 1, pp. 17–32, Feb. 2003.
- [6] Q. Li, H. Li, J. Russell, P., Z. Chen, and C. Wang, "Ca-p2p: context-aware proximity-based peer-to-peer wireless communications," *Communications Magazine, IEEE*, vol. 52, no. 6, pp. 32–41, June 2014.
- [7] M. Großmann, "Proximity enhanced mobile d2d video streaming," in *Proceedings of the 18th Annual International Conference on Mobile Computing and Networking (Mobicom '12)*, 2012, pp. 427–430.
- [8] J. Kim, F. Meng, P. Chen, H. E. Egilmez, D. Bethanabhotla, A. F. Molisch, M. J. Neely, G. Caire, and A. Ortega, "Adaptive video streaming for device-to-device mobile platforms," in *Proceedings of the 19th Annual International Conference on Mobile Computing Networking (MobiCom '13)*, 2013, pp. 127–130.
- [9] V. Ayadurai and M. Prytz, "Software radio platform for network-assisted device-to-device (na-d2d) concepts," in *Proceedings of the Second Workshop on Software Radio Implementation Forum (SRIF 13')*, 2013, pp. 53–60.
- [10] M. Corson, R. Laroia, J. Li, V. Park, T. Richardson, and G. Tsirtsis, "Toward proximity-aware internetworking," *IEEE Wireless Communications*, vol. 17, no. 6, pp. 26–33, December 2010.
- [11] X. Wu, S. Tavildar, S. Shakkottai, T. Richardson, J. Li, R. Laroia, and A. Jovicic, "Flashlinq: A synchronous distributed scheduler for peer-to-peer ad hoc networks," *IEEE/ACM Trans. Netw.*, vol. 21, no. 4, pp. 1215–1228, Aug. 2013.
- [12] M. Zulhasnine, C. Huang, and A. Srinivasan, "Exploiting cluster multicast for p2p streaming application in cellular system," in *IEEE Wireless Communications and Networking Conference (WCNC)*, April 2013, pp. 4493–4498.
- [13] Y. Shen, W. Zhou, P. Wu, L. Toni, P. Cosman, and L. Milstein, "Device-to-device assisted video transmission," in *Proceedings of the 20th International Packet Video Workshop (PV)*, Dec 2013, pp. 1–8.
- [14] B. Kaufman, J. Lilleberg, and B. Aazhang, "Spectrum sharing scheme between cellular users and ad-hoc device-to-device users," *IEEE Trans. Wireless Commun.*, vol. 12, no. 3, pp. 1038–1049, March 2013.
- [15] P. Jänis, C.-H. Yu, K. Doppler, C. Ribeiro, C. Wijting, K. Hugl, O. Tirkkonen, and V. Koivunen, "Device-to-device communication underlying cellular communication systems," *International Journal on Communications, Network and System Science*, 2009.
- [16] C.-H. Yu, K. Doppler, C. Ribeiro, and O. Tirkkonen, "Resource sharing optimization for device-to-device communication underlying cellular networks," *IEEE Trans. Wireless Commun.*, vol. 10, no. 8, pp. 2752–2763, August, 2011.
- [17] H. Min, J. Lee, S. Park, and D. Hong, "Capacity enhancement using an interference limited area for device-to-device uplink underlying cellular networks," *IEEE Trans. Wireless Commun.*, vol. 10, no. 12, pp. 3995–4000, 2011.
- [18] J. Wang, D. Zhu, C. Zhao, J. Li, and M. Lei, "Resource sharing of underlying device-to-device and uplink cellular communications," *IEEE Communications Letters*, vol. 17, no. 6, pp. 1148–1151, 2013.
- [19] D. Feng, L. Lu, Y. Yuan-Wu, G. Li, G. Feng, and S. Li, "Device-to-device communications underlying cellular networks," *Communications, IEEE Transactions on*, vol. 61, no. 8, pp. 3541–3551, August 2013.
- [20] D. H. Lee, K. W. Choi, W. S. Jeon, and D. G. Jeong, "Two-stage semi-distributed resource management for device-to-device communication in cellular networks," *IEEE Trans. Wireless Commun.*, vol. 13, no. 4, pp. 1908–1920, April 2014.
- [21] Y. Wu, S. Wang, W. Guo, X. Chu, and J. Zhang, "Optimal resource management for device-to-device communications underlying sc-fdma

- system,” in *9th IEEE/IET International Symposium on Communication Systems, Networks and Digital Signal Processing*, July 2014.
- [22] M. Cha, H. Kwak, P. Rodriguez, Y.-Y. Ahn, and S. Moon, “I tube, you tube, everybody tubes: Analyzing the world’s largest user generated content video system,” in *Proceedings of the 7th ACM SIGCOMM Conference on Internet Measurement*, 2007, pp. 1–14.
- [23] M. N. Tehrani, M. Uysal, and H. Yanikomeroglu, “Device-to-device communication in 5g cellular networks: challenges, solutions, and future directions,” *IEEE Commun. Mag.*, vol. 52, no. 5, pp. 86–92, May 2014.
- [24] P. Li and S. Guo, “Incentive mechanisms for device-to-device communications,” *IEEE Network*, vol. 29, no. 4, pp. 75–79, July 2015.
- [25] C. Buragohain, D. Agrawal, and S. Suri, “A game theoretic framework for incentives in p2p systems,” in *Proceedings of IEEE International Conf. Peer-to-Peer Computing (P2P 2003)*, Sept 2003, pp. 48–56.
- [26] C.-H. Lin, S.-A. Yuan, S.-W. Chiu, and M.-J. Tsai, “Progressface: An algorithm to improve routing efficiency of gpsr-like routing protocols in wireless ad hoc networks,” *IEEE Trans. on Comput.*, vol. 59, no. 6, pp. 822–834, Jun. 2010.
- [27] D. W. K. Ng, E. S. Lo, and R. Schober, “Dynamic resource allocation in mimo-ofdma systems with full-duplex and hybrid relaying,” *IEEE Transactions on Communications*, vol. 60, no. 5, pp. 1291–1304, 2012.
- [28] G. TSG-RAN, “Further advancements for e-utra physical layer aspects,” 3GPP Technical Report, 3G TR 36.814 v9.0.0, Mar. 2010.
- [29] E. J. O’neil, P. E. O’Neil, G. Weikum, and E. Zurich, “The lru-k page replacement algorithm for database disk buffering,” in *ACM SIGMOD International Conference on Management of Data*, 1993, pp. 297–306.
- [30] L. Lei, Z. Zhong, C. Lin, and X. Shen, “Operator controlled device-to-device communications in lte-advanced networks,” *IEEE Wireless Commun. Mag.*, vol. 19, no. 3, pp. 96–104, June 2012.
- [31] P. M. Pardalos and J. B. Rosen, *Constrained Global Optimization: Algorithms and Applications*. Springer Berlin Heidelberg, 1987.
- [32] J. E. Falk and R. M. Soland, “An algorithm for separable nonconvex programming problems,” *Management Science*, vol. 15, no. 9, pp. 550–569, 1969.
- [33] E. Süli and D. F. Mayers, *An Introduction to Numerical Analysis*. Cambridge University Press, 2003.
- [34] H. P. Benson, “Separable concave minimization via partial outer approximation and branch and bound,” *Operations Research Letters*, vol. 9, no. 6, pp. 389–394, Nov. 1990.
- [35] A. E. Gamal and Y.-H. Kim, *Network Information Theory*. Cambridge University Press, 2011.